Original Works

Evaluation of the degree of liver damage by dynamic MRI using ferucarbotran

Terutoshi Masunami

Department of Radiology,
*Kyoto Prefectural University of Medicine Graduate School of Medical Science**

Abstract: Purpose: To determine whether SPIO-enhanced dynamic MRI can be used to assess the degree of liver dysfunction.

Material and methods: The subjects were 41 patients with liver disease. Dynamic studies were performed with bolus injection of ferucarbotran, and arterial- and portal-phase images were obtained. T2- and T2*-weighted images were also obtained 10 min after injection. We compared the degree of liver dysfunction determined using blood markers with the degree of signal changes in MRI.

Results: Relative signal intensity of arterial-phase images was 0.42±0.05 in patients with normal liver function, 0.75±0.22 in those with mild dysfunction, and 0.88±0.08 in those with severe dysfunction. The difference between each group was statistically significant ($p<0.050$). A similar trend was noted for portal-phase images, T2-weighted images, and T2*-weighted images. The degree of signal change was the largest in the T2*-weighted images, but the difference between the normal group and the mild and severe dysfunction groups was the most clear using arterial-phase images.

Conclusion: Dynamic MRI may be useful in assessing liver function. The differences were particularly well depicted using arterial-phase and T2*-weighted images.

Key words: MRI, SPIO, Ferucarbotran, Dynamic, Liver damage.

Introduction

Superparamagnetic iron oxide (SPIO) is a magnetic resonance (MR) contrast agent designed to assess phagocytotic activity in the liver, and its clinical utility has been established in several studies[1-6]. Up to 80% of the injected contrast agent is taken up by Kupffer cells in liver sinusoids, where its particles form large clusters. SPIO clusters cause substantial perturbation of the magnetic field, resulting in marked T2 shortening of liver parenchyma[7]. The activity and number of Kupffer cells may therefore be directly related to the signal changes induced by SPIO in T2- or T2*-weighted images[14)15)]. Several studies found less significant alteration of signal in the liver after SPIO administration when

Received: January 27, 2009. Accepted: January 30, 2009 * Address for correspondence: *465 Kajii-cho, Kawaramachi-Hirokoji, Kamigyo-ku, Kyoto 602-8566, Japan*

patients with acute and chronic hepatitis were imaged, and concluded that SPIO phagocytosis was disturbed in these patients[8-13].

Liver function test by blood sampling is the most widely used method to estimate liver function. However, it cannot identify the geographic distribution of liver damage. MRI is much more advantageous in terms of such spatial localization, and the SPIO technique allows qualitative assessment of focal liver lesions and liver dysfunction. Such assessment of liver function may be crucial when planning resection or transplantation of the liver.

Recent studies have used perfusion MRI or CT techniques, and indicated that the perfusion deficit of the liver can be visualized using these techniques. Earlier, the available SPIO agent (ferumoxide) was not designed for bolus injection and MRI equipment was not sufficiently developed to carry out high-speed and high-resolution imaging techniques, including echo-planar imaging[16]. The newer SPIO agent ferucarbotran can be used for bolus injection; MRI equipment and imaging techniques have improved; and high-performance gradient systems and parallel imaging techniques are available. This has enabled assessment of liver perfusion with SPIO.

We carried out a dynamic study of the liver to assess liver function assuming that the technique would reflect the viability of Kupffer cells and perfusion status of the liver. The purpose of this study was to determine whether dynamic scans of the liver can be used to evaluate liver function.

Patients and methods

Patient population

This study was approved by our institutional review board. Written informed consent was obtained from each patient.

Forty-one (28 males and 13 females) consecutive patients (mean age, 62 years; range, 31-80 years) underwent MRI using a fixed protocol from October 2004 to April 2005. Five patients with normal liver function were imaged for metastatic liver tumor. A second group of patients had mild liver dysfunction (chronic hepatitis; n=20) and the third group had severe liver dysfunction (liver cirrhosis; n=16). Severity of liver dysfunction was diagnosed using routine laboratory tests and liver biopsy. Fibrosis scores classified F1 or F2 with mild liver dysfunction, and F3 or F4 with severe liver dysfunction. Laboratory tests classified type Ⅳ collagen 7S (<8.0 ng/ml) with mild liver dysfunction, and type Ⅳ collagen 7S (≧8.0 ng/ml) with severe liver dysfunction. Patient groups were classified into viral hepatitis (n=33) versus alcoholic hepatitis (n=3).

MRI

Images were obtained with a 1.5-Tesla whole-body scanner (Gyroscan Intera, Philips, Best, The Netherlands). T2-weighted images were SE with TR=2400, TE=70, TSE factor=23, and matrix size =512×256. T2*-weighted images were fast-field echo (FFE) with TR=400, TE=14, flip angle=35°, and matrix size =512×256. Dynamic images were obtained by single-shot EPI with TR=1600, TE=72, EPI factor=39, flip angle=90°, and matrix size=256×192. The entire liver was covered with 20 trans-axial slices (thickness, 7 mm). The contrast agent ferucarbotran (0.016 ml/kg) was injected with a mechanical injector (Spectris, MedRad, PA, USA) at a rate of 2.0 ml/s into an antecubital vein.

Dynamic liver scans were started immediately after injection. One slice per second was taken for 25 s (arterial phase). After 10 s, the same process was repeated for another set of 25 s (portal phase). T2-weighted and T2*-weighted images were obtained approximately 10 min after completion of

dynamic scans.

Data analysis

Region of interest (ROI) analysis was done using a single circular ROI placed at the liver tissue 1 cm lateral to the right portal vein (Figs. 1-3). Non-contrast scans were used as the first phase of the dynamic study and as baseline control for the rest of the images. Relative signal changes in each dynamic scans were calculated from this baseline ROI:

(Pre-contrast signal−Post-contrast signal)/Pre-contrast signal

We placed the ROI at other slices, using the right portal vein as an anatomic reference, if there was motion due to poor holding of breath. We did similar measurements on T2- and T2*-weighted images by placing the ROI at the same location. Signal changes were calculated using the paraspinal muscles as the control location.

Measurements were done at three locations in each patient to confirm that the ROI placements had avoided areas with artifacts.

Statistical analysis was carried out using Student's *t*-test for each group.

Fig. 1

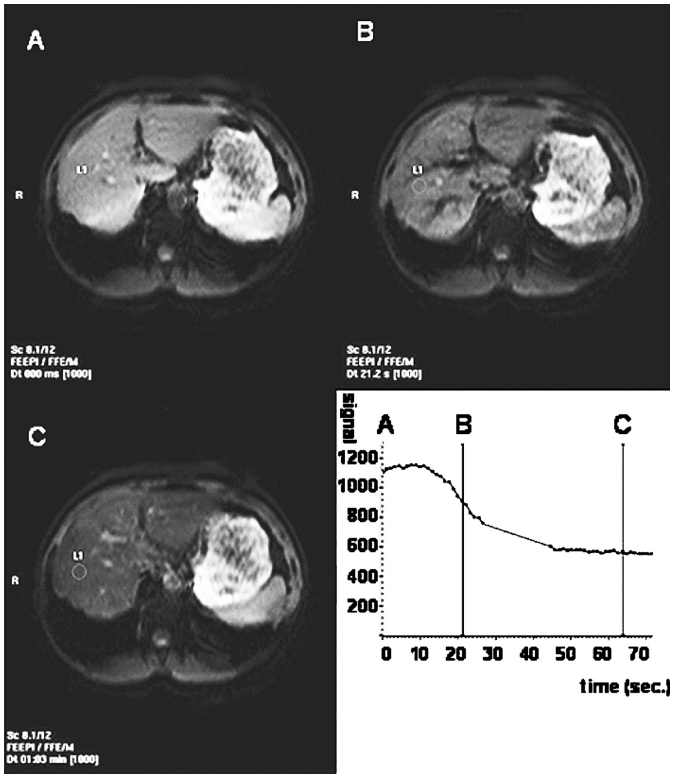

Fig. 1 - 3. Typical MRI and time-intensity curve for the dynamic scans with normal liver function (Fig. 1), mild liver dysfunction (Fig. 2), and severe liver dysfunction (Fig. 3) after resovist injection (0.016 ml/kg). A linear part in the center of the time-intensity curve is rest time between the arterial and portal phase.

Fig. 2

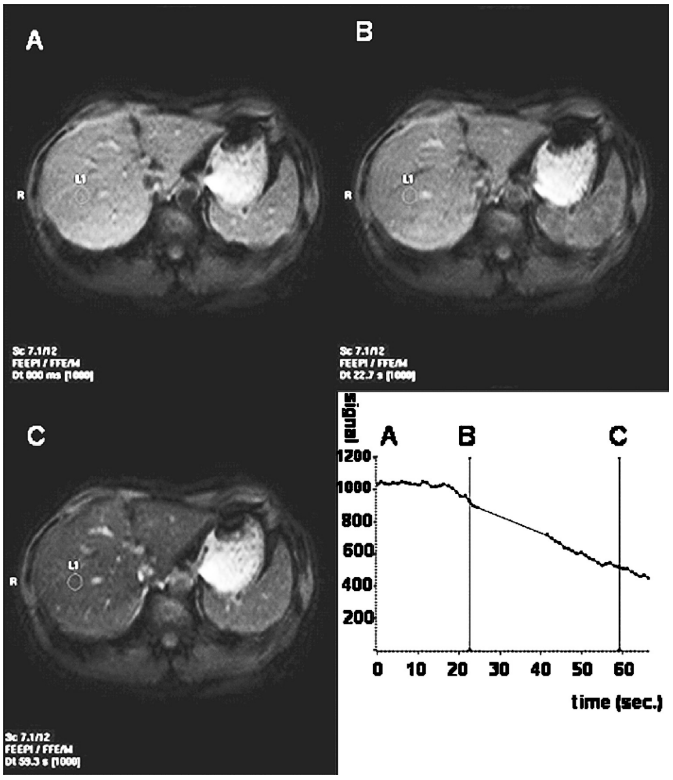
A
B
C
R
L1
signal
time (sec.)
0 10 20 30 40 50 60
200 400 600 800 1000 1200

Fig. 3

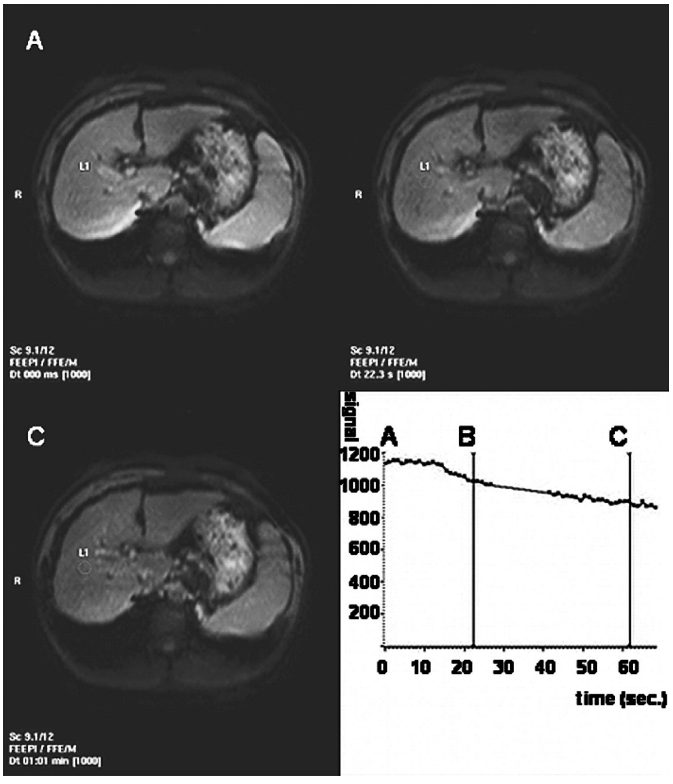
A
B
C
R
L1
signal
time (sec.)
0 10 20 30 40 50 60
200 400 600 800 1000 1200

Results

Signal changes induced by bolus administration of SPIO are described below.

Plots of the arterial and portal phases are illustrated in Figs. 4 and 5, respectively. Time 0 was defined as the time when the contrast agent reached the abdominal aorta at the level of the celiac artery. There were no significant differences between the three groups in the early arterial phase, but the differences grew larger in the late arterial phase that was 25 sec after injection ($p<0.01$). We therefore chose to use this late arterial phase to compare the results with other sequences.

Statistical significance was noted at all times for the portal phase, but the difference appeared to be largest at the later phase. We therefore used the late portal phase that was 60 sec after injection for comparison.

Relative signal changes in the arterial phase were 0.42 ± 0.05, 0.75 ± 0.22, and 0.88 ± 0.08 for normal, mild, and severe liver dysfunction, respectively. Relative signal changes in the portal phase were 0.34 ± 0.06, 0.54 ± 0.08, and 0.72 ± 0.11 for normal, mild, and severe liver dysfunction, respectively (Fig. 6).

Signal changes at 10 min for T2-weighted images were 0.38 ± 0.03, 0.49 ± 0.07, and 0.64 ± 0.13 for normal, mild, and severe liver dysfunction, respectively. Signal changes at 10 min for T2*-weighted images were 0.09 ± 0.02, 0.20 ± 0.06, and 0.34 ± 0.11 for normal, mild, and severe liver dysfunction, respectively (Fig. 6).

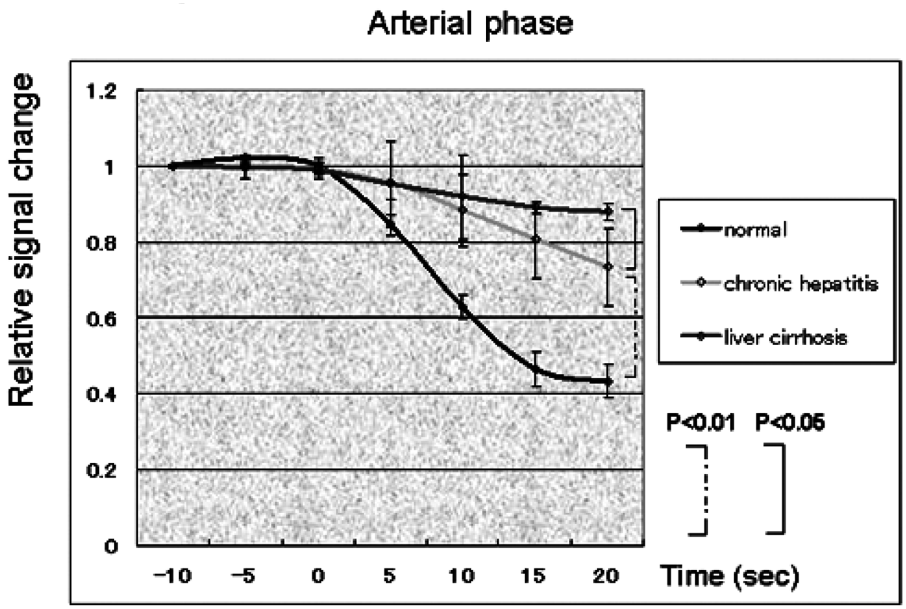

Fig. 4. Relative signal changes of the liver at arterial phase after injection of resovist in normal function, mild liver dysfunction, and severe liver dysfunction.

A significant difference in relative signal changes is noted in the late arterial phase between normal function, mild dysfunction, and severe dysfunction ($P<0.05$, each group by Student's *t*-test).

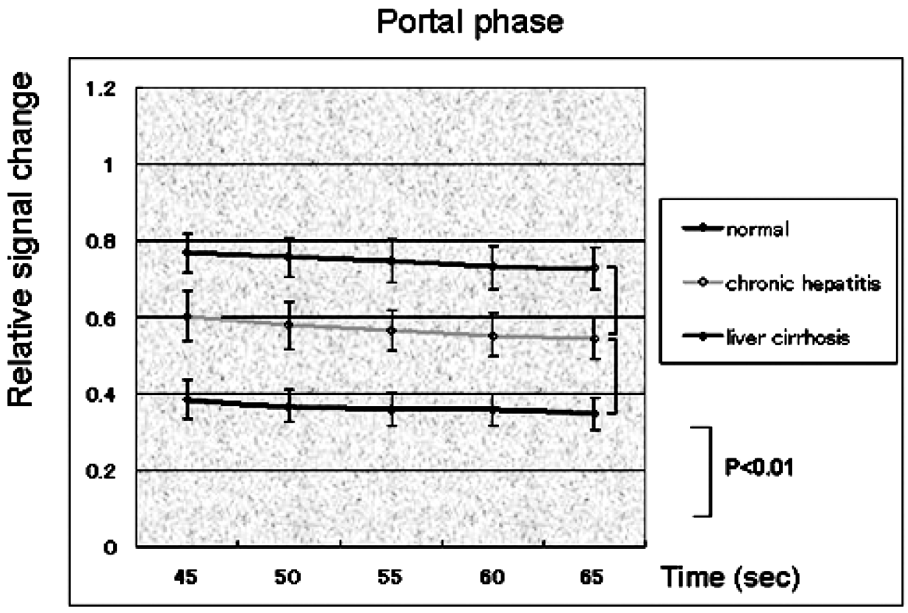

Fig. 5. Relative signal changes of the liver at portal phase after injection of resovist in normal function, mild liver dysfunction, and severe liver dysfunction.

A significant difference in relative signal changes is noted in the leach late portal phase between normal function, mild dysfunction, and severe dysfunction ($P<0.01$, each group by Student's *t*-test).

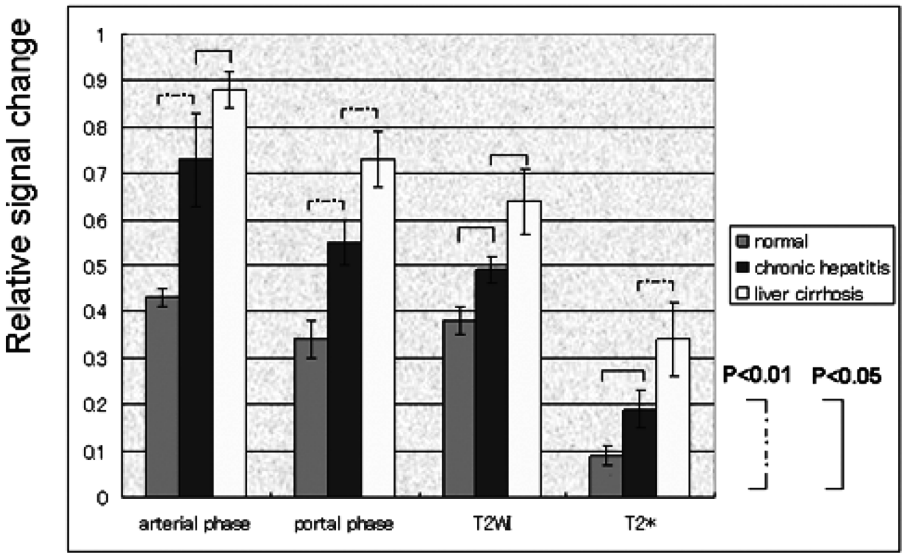

Fig. 6. Relative signal changes of the liver at late arterial-phase, late portal-phase, T2-, and T2*-weighted images after injection of resovist in normal function, mild liver dysfunction, and severe liver dysfunction.

A significant difference in relative signal changes is noted in each phase between normal function, mild dysfunction, and severe dysfunction ($P<0.05$, each group by Students *t*-test).

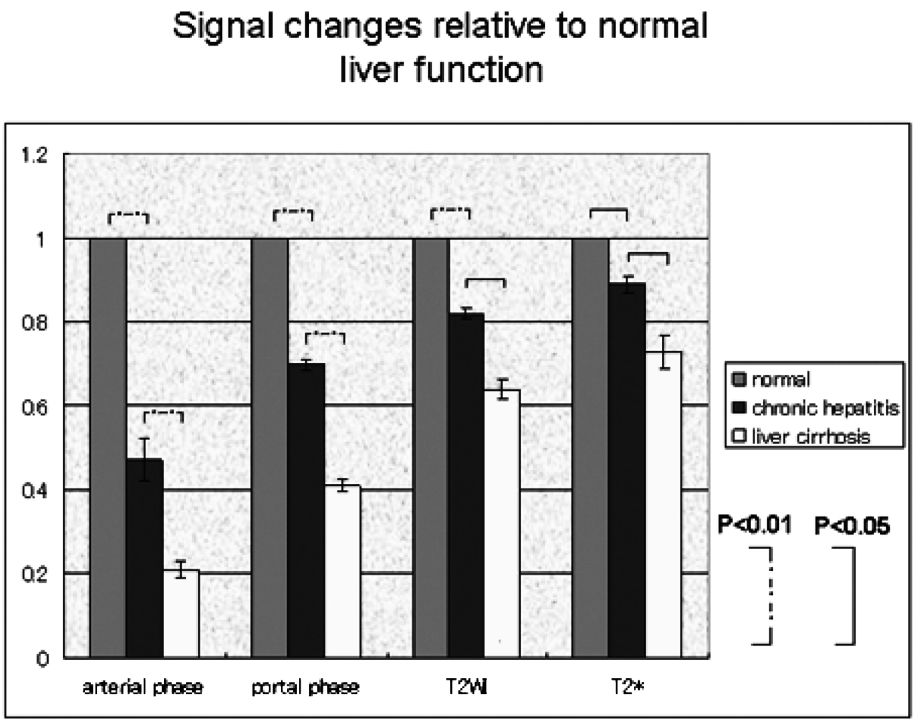

Fig. 7. The difference between normal function, and mild and severe liver dysfunction was the largest in the late arterial-phase images, although the signal decrease was the largest in T2*-weighted images in each group.

There were significant differences ($p<0.05$) for all sequences between these groups. Highest signal changes were seen for T2*-weighted images.

We further analyzed the data to examine which of the imaging methods had the highest change in signal relative to the normal group. The signal change of the normal liver function group was defined as 1. The relative signal change was 0.43 ± 0.044 and 0.21 ± 0.016 in arterial-phase images; 0.70 ± 0.013 and 0.42 ± 0.018 in portal-phase images; 0.82 ± 0.023 and 0.58 ± 0.043 in T2-weighed image; and 0.89 ± 0.03 and 0.73 ± 0.055 in T2*-weighted images, for the mild and severe liver dysfunction groups, respectively (Fig. 7).

The change in signal between the normal and liver dysfunction groups was the highest for the arterial phase of dynamic MRI (although signal decrease was the largest for each group in T2*-weighted images). The second highest signal change was in the portal phase of dynamic MRI.

Discussion

We demonstrated that all T2/T2*-weighted images could show different degrees of signal change depending on the degree of liver damage. These differences were statistically significant for all imaging methods. The arterial-phase images obtained by the dynamic scan method demonstrated the largest signal differences between the groups. This indicates that the dynamic scan method was the best method for evaluating severity of liver damage.

We assumed that the delayed scans (T2-/T2*-weighted images) taken 10 min after injection were not related to the degree of decrease in blood flow but simply reflected the phagocytotic ability of Kupffer cells. Dynamic scans probably reflected liver perfusion, thereby differentiating differences between mild and severe damage.

Signal loss observed within the liver tissue during bolus injection of SPIO may reflect two different classes of pathophysiology: (i) the amount of the contrast agent reaching the liver (perfusion term); and (ii) the clustering of SPIO taken-up within Kupffer cells. The less change in signal in the poor liver function group probably reflects deficit in perfusion and phagocytosis.

Recent research has shown that if liver damage occurs, not only the total amount of blood flow decreases but also the ratio between arterial and portal flow is altered. Relative increase in arterial blood flow occurs as liver damage progresses, whereas the portal flow declines. There was only a minor difference between the mild versus severe liver damage groups on arterial-phase images, which may indicate that increased arterial blood flow was a compensation mechanism. The difference between mild versus severe groups was larger for the portal phase, suggesting that the decline in portal flow accelerated the difference.

It has been advocated that T2- and T2*-weighted images should be obtained>10 min after contrast injection. We found that dynamic-phase data was the most sensitive in assessing the degree of liver damage.

MRI assessment of liver function may be crucial, for example, when planning liver resection for patients with hepatic failure because the geographic distribution of liver function reserve must be assessed. When planning liver transplantation, liver function reserve of the donor may become important to lessen the risk of postoperative liver function failure or to increase the chance of long-term survival. Our method may provide more information than the conventional volume measurements of the liver.

The SPIO technique is an established imaging method that allows qualitative assessment of focal liver lesions, and additional information derived from dynamic SPIO imaging may increase the value of this test.

There were limitations in this study. First, slice location will always hamper accurate estimation of signal change (it is a problem for other imaging techniques involving holding the breath). This made ROI analysis difficult in some cases. A certain degree of spatial misregistration is unavoidable; however, subtle location differences will not be a substantial problem because we are dealing with patients with diffuse liver damage. Second, the artifact at the lateral segment of the left lobe cannot be avoided because it is induced by cardiac pulsation as well as diaphragmatic motion. Our technique is therefore limited to other parts of the liver. Third, we could not obtain liver biopsy in all cases. We used not only the blood liver function test, but also relied on some fibrosis markers, including type Ⅳ collagen 7S and hyaluronic acid, to overcome this issue. There was high correlation between these markers and biopsy-graded degree of liver fibrosis[17-20]. We believe that correlation with these markers is sufficient.

In conclusion, high resolution dynamic MRI may be useful in assessing liver function. The differences were especially well depicted using arterial-phase T2*-weighted images.

References

1) Josephson L, Lewis J, Jacobs P, Hahn PF, Stark DD. The effects of iron oxide on proton elaxivity. Magn Reson Imaging 1988; 6: 647-653.

2) Majumdar S, Gore JC. Studies of diffusion in random fields produced by variations in susceptibility. J Magn Reson 1988; 78: 41-55.

3) Kawamura Y, Endo K, Watanabe Y, et al. Use of magnetite particles as a contrast agent for MR imaging of the liver. Radiology 1990; 174: 357-360.

4) Muller RN, Gillis P, Moiny F, Roch A. Transverse relaxivity of particulate MRI contrast media: from theories to experiments. Magn Reson Med 1991; 22: 178-182.

5) Tanimoto A, Pouliquen D, Kreft BP, Stark DD. Effects of spatial distribution on proton relaxation enhancement by particulate iron oxide. J Magn Reson Imaging 1994; 4: 653-657.

6) Josephson L, Groman EV, Menz E, Lewis JM, Bengele H. A functionalized superparamagnetic iron oxide colloid as a receptor directed MR contrast agent. Magn Reson Imaging 1990; 8: 637-646.

7) Tanimoto A, Oshio K, Suematsu M, Pouliquen D, Stark DD. Relaxation effects of clustered particles. J Magn Reson Imaging 2001; 14: 72-77.

8) Murakami T, et al. Evaluation of regional liver damage by magnetic resonance imaging with superparamagnetic iron oxide in rat liver. Dig Dis Sci 2001; 46(1): 148-155.

9) Muhler A, et al. Acute liver rejection: evaluation with cell-directed MR contrast agents in a rat transplantation model. Radiology 1993; 186(1): 139-46.

10) Elizondo G, Weissleder R, Stark DD, et al. Hepatic cirrhosis and hepatitis: MR imaging enhanced with superparamagnetic iron oxide. Radiology 1990; 174: 797-801.

11) Yamashita Y, Yamamoto H, Hirai A, Yoshimatsu S, Baba Y, Takahashi M. MR imaging enhancement with superparamagnetic iron oxide in chronic liver disease: influence of liver dysfunction and parenchymal pathology. Abdom Imaging 1996; 21: 318-323.

12) Kreft B, Block W, Dombrowski F, et al. Diagnostic value of a superparamagnetic iron oxide in MR imaging of chronic liver disease in an animal model. AJR Am J Roentgenol 1998; 170: 661-668.

13) Kato N, Ihara S, Tsujimoto T, Miyazawa T. Effect of resovist on rats with different severities of liver cirrhosis. Invest Radiol 2002; 37: 292-298.

14) Lucidarme O, Baleston F, Cadi M, et al. Non-invasive detection of liver fibrosis: Is superparamagnetic iron oxide particle-enhanced MR imaging a contributive technique? Eur Radiol 2003; 13: 467-474.

15) Tanimoto A, Mukai A, Kuribayashi S. Evaluation of Superparamagnetic Iron Oxide for MR Imaging of Liver Injury: Proton Relaxation Mechanisms and Optimal MR Imaging Parameters. Magnetic Resonance in Medical Sciences 2006; 5(2): 89-98.

16) Ichikawa T, et al. Perfusion MR imaging with a superparamagnetic iron oxide using T2-weighted and susceptibility-sensitive echoplanar sequences: evaluation of tumor vascularity in hepatocellular carcinoma. AJR Am J Roentgenol 1999; 173(1): 207-13.

17) Murawaki Y, Ikuta Y, Koda M, Kawasaki H. Serum type Ⅲ procollagen peptide, type Ⅳ collagen 7S domain, central triple helix of type Ⅳ collagen and tissue inhibitor of metalloproteinases in patients with chronic viral liver disease:Relationship to liver histology. Hepatology 1994; 20: 780-787.

18) Suou T, Yamada S, Hosho K, et al. Relationship between serum and hepatic 7S fragments of type Ⅳ collagen in chronic liver disease. Hepatology 1996; 23: 1154-1158.

19) Yamada S, Suou T, Kawasaki H, Yoshikawa N. Clinical significance of serum 7S collagen in various liver diseases. Clin Biochem 1992; 25: 467-470.

20) Kawai S, Kubo S, Tadashi T, et al. Serum concentration of type Ⅳ collagen 7S domain as a marker for increased risk of recurrence after liver resection for hepatocellular carcinoma. Dig Surg 2003; 20(3): 201-208.

＜和文抄録＞

フェルカルボトランを用いたダイナミック MRI による肝障害の評価の検討

増　南　輝　俊

京都府立医科大学大学院医学研究科放射線治療診断学

【目的】

SPIO 造影 dynamic MRI を撮像し，肝実質信号変化と肝障害との関係を検討した．

【方法・対象】

対象は正常群 5 例，軽症肝障害群 20 例，重症肝障害群 16 例の 41 症例．SPIO 造影剤（ferucarbotran）を注入直後に，dynamic MRI（動脈相および門脈相）の撮像を行い，T2WI と T2*は注入後 10 分で撮像を行った．肝障害の程度に対する SPIO 造影 MRI での信号変化と血液生化学所見の比較を行った．

【結果】

造影剤投与前の信号強度を 1 として，動脈相の信号強度は，正常群 0.42±0.05，軽症群 0.75±0.22，重症群 0.88±0.08 となり，各群間に有意差（$p<0.05$）を認めた．同様に門脈層，T2WI，T2*においても各群間に有意差（$p<0.05$）を認めた．信号低下率では T2*が各群において最大であったが，正常群と肝障害群の信号低下率の比では，動脈相が最大であった．

【結論】

SPIO 造影 dynamic MRI は肝機能の評価に有用であると考える．

キーワード：MRI，SPIO，Ferucarbotran，肝障害．